

The effect of the boundary slip on the stability of shear flow

Qiaolin He and Xiao-Ping Wang

Department of Mathematics, The Hong Kong University of Science and Technology, Clear Water Bay, Kowloon, Hong Kong

Received 24 January 2008, accepted 12 June 2008

Published online 10 September 2008

Key words Orr-Sommerfeld equation, stability, Navier slip boundary condition, shear flow.

MSC (2000) 33F05, 34K20, 34L16, 76E05, 76F10

We study the linearized stability of shear flow satisfying Navier slip boundary conditions. The Orr-Sommerfeld equation for the plane Poiseuille flow with Navier slip boundary conditions is solved numerically by the Chebyshev collocation method. Our numerical results show that slip at the boundary increases the critical Reynolds number R_c for instability. The dependence of the this critical Reynolds number on the slip length l_s is found to be $R_c(l_s) - R_c(0) \approx Cl_s^2$.

Z. Angew. Math. Mech. **88**, No. 9, 729–734 (2008) / DOI 10.1002/zamm.200800020

www.zamm-journal.org

The effect of the boundary slip on the stability of shear flow

Qiaolin He* and Xiao-Ping Wang

Department of Mathematics, The Hong Kong University of Science and Technology, Clear Water Bay, Kowloon, Hong Kong

Received 24 January 2008, accepted 12 June 2008

Published online 10 September 2008

Key words Orr-Sommerfeld equation, stability, Navier slip boundary condition, shear flow.

MSC (2000) 33F05, 34K20, 34L16, 76E05, 76F10

We study the linearized stability of shear flow satisfying Navier slip boundary conditions. The Orr-Sommerfeld equation for the plane Poiseuille flow with Navier slip boundary conditions is solved numerically by the Chebyshev collocation method. Our numerical results show that slip at the boundary increases the critical Reynolds number R_c for instability. The dependence of the this critical Reynolds number on the slip length l_s is found to be $R_c(l_s) - R_c(0) \approx Cl_s^2$.

© 2008 WILEY-VCH Verlag GmbH & Co. KGaA, Weinheim

1 Introduction

The Orr-Sommerfeld equation, in fluid dynamics, is an eigenvalue equation describing the linear two-dimensional modes of disturbance to a viscous parallel flow where the no-slip boundary condition is usually assumed. For all but the simplest of velocity profiles, numerical or asymptotic methods are required to calculate solutions. For Poiseuille flow, it has been shown that the flow is unstable when Reynolds number $R > R_c = 5772.22$ [2].

It is well known that in many fluid regimes, the slip of the fluid at the solid boundary becomes important, for example, for the micro-channel flow [9], the driven cavity flow [11] and the moving contact line problem [10]. A nature question to ask is how the slip at the boundary affects the stability of the Poiseuille flow. In another word, will allowing slip increase or decrease the critical Reynolds number $R_c = 5772.22$. A numerical study by Chu [6] suggested that the velocity-slip at the wall will degrade the stability of the flow. That is, the relaxed slip-flow effect decreases the critical Reynolds number.

In this paper, we carry out a careful numerical study of the Orr-Sommerfeld equation with the Navier slip boundary condition. Our results suggest the opposite, that is, the critical Reynolds number R_c increases with the slip length l_s . Therefore, allowing slip increases the stability of the shear flow. Moreover, we have $R_c(l_s) - R_c(0) \approx Cl_s^2$. Here $R_c(0)$ is the critical Reynolds number with the no-slip boundary condition.

2 Mathematical model

The two dimensional Navier-Stokes equations for an incompressible fluid flow are

$$\frac{\partial \mathbf{u}}{\partial t} + (\mathbf{u} \cdot \nabla) \mathbf{u} + \nabla p = \frac{1}{R} \Delta \mathbf{u}, \quad (2.1)$$

$$\nabla \cdot \mathbf{u} = 0, \quad (2.2)$$

where R is the Reynolds number. In studying the linearized stability of the basis shear flow $U(y)$, a usual assumption is

$$u(x, y, t) = U(y) + u'(x, y, t),$$

$$v(x, y, t) = v'(x, y, t),$$

$$p(x, y, t) = \text{constant} + p'(x, y, t),$$

where u' and v' are the components of disturbance velocity. Using normal-mode decomposition analysis, a stream function for the disturbance, ψ' is assumed to have the form

$$\psi'(x, y, t) = \phi(y)e^{i\alpha(x-ct)},$$

* Corresponding author, e-mail: hqlaa@ust.hk

where ψ' is defined such that $u' = \psi'_y$ and $v' = -\psi'_x$. After linearizing and rewriting the equations of vorticity of 2-dimensional disturbance, we obtain the famous Orr-Sommerfeld equation

$$\begin{aligned} (i\alpha R)^{-1}(D^2 - \alpha^2)^2\phi &= (U - c)(D^2 - \alpha^2)\phi - U''\phi, \\ L\phi + cM\phi &= 0, \end{aligned} \quad (2.3)$$

where $D = \frac{\partial}{\partial y}$, and

$$\begin{aligned} L &= (i\alpha R)^{-1}(D^2 - \alpha^2)^2 - \{U(D^2 - \alpha^2) - U''\}, \\ M &= D^2 - \alpha^2. \end{aligned}$$

For plane Poiseuille flow with no-slip boundary conditions $\phi = D\phi = 0$, (2.3) is an eigenvalue problem for $c = c_r + ic_i$. Therefore we have stability if all $c_i < 0$, instability if there exist a $c_i > 0$ and the neutral stability if at least one $c_i = 0$, the remaining c_i having vanishing or negative imaginary parts. The eigenvalue problem (2.3) with no-slip boundary conditions was solved by Orszag [2] who predicts a critical Reynolds number $R = 5772.22$ at which instability should first occur.

We now consider the same problem with the Navier slip boundary condition. The basic flow we shall consider is now given by

$$U(y) = 1 - y^2 + 2l_s \quad (2.4)$$

for $-1 \leq y \leq 1$. It is easy to see that U satisfies (2.1)–(2.2) as well as the Navier boundary conditions

$$l_s^{-1}U = -\partial_n U$$

at $y = \pm 1$. In terms of stream function ϕ , the Navier slip boundary conditions are in the following form,

$$\begin{aligned} \phi = 0, \quad l_s^{-1}\phi' &= \phi'' \quad \text{at } y = -1, \\ \phi = 0, \quad l_s^{-1}\phi' &= -\phi'' \quad \text{at } y = 1. \end{aligned} \quad (2.5)$$

3 Numerical method

We solve the eigenvalue problem for the Eqs. (2.3)–(2.4) and its associated boundary conditions (2.5) by Chebyshev collocation method [13]. Consider the set of Chebyshev nodes $\{x_k\}$ with endpoints $x = \pm 1$,

$$x_k = \cos\left(\frac{(k-1)\pi}{N-1}\right), \quad k = 1, \dots, N. \quad (3.1)$$

and the corresponding Lagrangian basis set $\{\xi_k(x)\}$,

$$\xi_k(x) = \frac{(-1)^k}{c_k} \frac{1-x^2}{(N-1)^2} \frac{T'_{N-1}(x)}{x-x_k}, \quad (3.2)$$

where $c_1 = c_N = 2$ and $c_2 = \dots = c_{N-1} = 1$, $T_{N-1}(x)$ represents the Chebyshev polynomial of degree $N-1$. The interpolating polynomial is taken to be

$$p_{N-1}(x) = \sum_{j=2}^{N-1} \phi_j \xi_j(x).$$

This interpolation satisfies $p_{N-1}(\pm 1) = 0$. We require the Eq. (2.3) to be satisfied at the interior $N-4$ grid points:

$$\sum_{j=2}^{N-1} \phi_j L_j(x_k) + c \sum_{j=2}^{N-1} \phi_j M_j(x_k) = 0, \quad k = 3, \dots, N-2. \quad (3.3)$$

The Navier slip boundary conditions imply

$$\begin{aligned} l_s^{-1} \sum_{j=2}^{N-1} \phi_j \xi'_j(x_1) + \sum_{j=2}^{N-1} \phi_j \xi''_j(x_1) &= 0, \\ l_s^{-1} \sum_{j=2}^{N-1} \phi_j \xi'_j(x_N) - \sum_{j=2}^{N-1} \phi_j \xi''_j(x_N) &= 0. \end{aligned} \quad (3.4)$$

Eqs. (3.3)–(3.4) form a linear system of $N - 2$ equations, which can be reduced to the form $A\phi = cB\phi$, where $\phi = [\phi_3, \dots, \phi_{N-2}]^T$, A and B are both the $(N - 4) \times (N - 4)$ matrices. The eigenvalue c is then obtained by the Matlab function $\text{eig}(B^{-1}A)$.

Our numerical results are verified by the Gauss-Jackson-Noumerov finite-difference method [12], which is described as follows. The Orr-Sommerfeld equation is replaced by a difference equation using central difference approximations to the derivatives with a truncation error involving the eighth derivative, and the error is fourth order. From [12], taking $g = \phi - \frac{1}{6}h^2D^2\phi + \frac{h^4}{90}D^4\phi$, the difference equation for the Orr-Sommerfeld equation becomes

$$\begin{aligned} & \delta^4 g \left[\left(\frac{1}{h^4} - \frac{2\alpha^2}{12h^2} + \frac{\alpha^4}{360} \right) + i\alpha R \left\{ (1 - c - y^2 + 2l_s) \left(\frac{1}{12h^2} - \frac{\alpha^2}{360} \right) + \frac{2}{360} \right\} \right] \\ & + \delta^2 g \left[\left(-\frac{2\alpha^2}{h^2} + \frac{\alpha^4}{6} \right) + i\alpha R \left\{ (1 - c - y^2 + 2l_s) \left(\frac{1}{h^2} - \frac{\alpha^2}{6} \right) + \frac{2}{6} \right\} \right] \\ & + g[\alpha^4 + i\alpha R\{(1 - c - y^2 + 2l_s)(-\alpha^2) + 2\}] = 0, \end{aligned}$$

with the following Navier slip boundary conditions:

$$\begin{aligned} g + \frac{1}{6}\delta^2 g + \frac{1}{360}\delta^4 g &= 0 \quad \text{at } y = \pm 1, \\ \frac{1}{2h}\delta g &= l_s \frac{1}{h^2} \left(\delta^2 g + \frac{1}{12}\delta^4 g \right) \quad \text{at } y = -1, \\ \frac{1}{2h}\delta g &= -l_s \frac{1}{h^2} \left(\delta^2 g + \frac{1}{12}\delta^4 g \right) \quad \text{at } y = 1, \end{aligned}$$

where $\delta g = g(y + h) - g(y - h)$, $\delta^2 g = g(y + h) - 2g(y) + g(y - h)$, and $\delta^4 g = g(y + 2h) - 4g(y + h) + 6g(y) - 4g(y - h) + g(y - 2h)$. The resulting system of the above difference equations can be reduced to the form $Ag = cBg$.

4 Results and discussions

As a test case, we first solve the eigenvalue problem for $l_s = 0$ (no-slip boundary conditions) and compare the results with the benchmark results of Orszag [2] and Li and Widnall [7]. Table 1 shows the eigenvalue with the largest imaginary part (the most unstable mode) for the plane Poiseuille flow with the Reynolds number $R = 10000$, the perturbation wave number $\alpha = 1.0$. It is clear that the result converges to $c_r + ic_i = 0.23752649 + 0.00373967i$ as we increase the number of Chebyshev nodes up to 128. Our numerical results are further verified by the Gauss-Jackson-Noumerov method [12]. The results are shown in Table 2. Compared with the finite difference method, the Chebyshev method shows much better convergence rate at much lower cost.

We now turn to the case with Navier slip boundary conditions with $\alpha = 1.0$, $R = 10000$ and the slip length $l_s = 0.008$. Our numerical results reported in Table 3 show that the eigenvalue with greatest imaginary part converges to $\lambda = 0.24326044 + 0.00227066i$. The results are again verified by the finite difference method with the eigenvalue with greatest imaginary part converges to the same $\lambda = 0.24326044 + 0.00227066i$ (Table 4).

The above test cases have shown that our method gives convergent and consistent results. We are now ready to study the effect of the slip on the stability of the shear flow. We first repeat the calculations for the no-slip case. In Table 5, we report the values of λ for the most unstable mode with $\alpha_c = 1.02056$, $l_s = 0.0$ for Reynolds numbers $R = 5772.22$ and $R = 5772.23$. The change of the sign for the imaginary part of the λ indicates that the Reynolds number is $R_c = 5772.22$, consistent with the previous results.

We now consider the slip boundary condition. For a fixed wave number $\alpha = 1.0$, we solve the eigenvalue problem for increasing Reynolds numbers and for four different slip length $l_s = 0.0, 0.005, 0.008, 0.01$. Fig. 1 plots the largest imaginary part C_i of eigenvalues as a function of the Reynolds number. It is clear that C_i becomes positive (i.e. the flow becomes unstable) for large enough Reynolds number. This critical Reynolds number increases with l_s indicating that the slip increases the stability of the flow. The critical Reynolds number also depends on the wave number α . For example, when $l_s = 0.008$, the most unstable wave number turns out to be $\alpha_c = 0.9922$ in which case the critical Reynolds number is the smallest. Our results in Table 6 show that the imaginary part of the λ changes sign between $R = 6410.91$ and $R = 6410.92$ indicating that the critical Reynolds number is $R_c = 6410.91$ which is much higher than the critical Reynolds number for the no-slip case.

Table 1 Approximation to the eigenvalue with largest imaginary part for $\alpha = 1.0$, $R = 10000$, $l_s = 0$, by the Chebyshev method.

grid points N	λ
32	$0.23741782 + 0.00375749i$
40	$0.23751460 + 0.00374111i$
48	$0.23752553 + 0.00374030i$
56	$0.23752644 + 0.00373971i$
64	$0.23752649 + 0.00373967i$
72	$0.23752649 + 0.00373967i$
80	$0.23752649 + 0.00373967i$
88	$0.23752649 + 0.00373967i$
96	$0.23752649 + 0.00373967i$
104	$0.23752649 + 0.00373967i$
112	$0.23752649 + 0.00373967i$
120	$0.23752649 + 0.00373967i$
128	$0.23752649 + 0.00373967i$

Table 2 Approximation to the eigenvalue with largest imaginary part for $\alpha = 1.0$, $R = 10000$, $l_s = 0$, by the finite difference method.

grid points N	λ
50	$0.23750060 + 0.00359250i$
100	$0.23752413 + 0.00373050i$
200	$0.23752633 + 0.00373910i$
300	$0.23752646 + 0.00373956i$
400	$0.23752648 + 0.00373964i$
500	$0.23752648 + 0.00373966i$
600	$0.23752649 + 0.00373966i$
700	$0.23752649 + 0.00373967i$
800	$0.23752649 + 0.00373967i$
900	$0.23752649 + 0.00373967i$
1000	$0.23752649 + 0.00373967i$

Table 3 Approximation to the eigenvalue with largest imaginary part for $\alpha = 1.0$, $R = 10000$, $l_s = 0.008$, by the Chebyshev method.

grid points N	λ
32	$0.24286430 + 0.00218839i$
40	$0.24319805 + 0.00230037i$
48	$0.24325588 + 0.00227719i$
56	$0.24326018 + 0.00227120i$
64	$0.24326042 + 0.00227068i$
72	$0.24326044 + 0.00227066i$
80	$0.24326044 + 0.00227066i$
88	$0.24326044 + 0.00227066i$
96	$0.24326044 + 0.00227066i$
104	$0.24326044 + 0.00227066i$
112	$0.24326044 + 0.00227066i$
120	$0.24326044 + 0.00227066i$
128	$0.24326044 + 0.00227066i$

Table 4 Approximation to the eigenvalue with largest imaginary part for $\alpha = 1.0$, $R = 10000$, $l_s = 0.008$, by the finite difference method.

grid points N	λ
50	$0.24331995 + 0.00217699i$
100	$0.24326377 + 0.00226462i$
200	$0.24326065 + 0.00227029i$
300	$0.24326048 + 0.00227058i$
400	$0.24326046 + 0.00227063i$
500	$0.24326045 + 0.00227065i$
600	$0.24326045 + 0.00227065i$
700	$0.24326044 + 0.00227066i$
800	$0.24326044 + 0.00227066i$
900	$0.24326044 + 0.00227066i$
1000	$0.24326044 + 0.00227066i$

Table 5 Approximation to the eigenvalue with largest imaginary part at the critical Reynolds number and wave number $\alpha_c = 1.02056$, when $l_s = 0.0$, by the Chebyshev method.

grid points N	$\lambda(R = 5772.22)$	$\lambda(R = 5772.23)$
20	$0.26234611 + 5.7i(-4)$	$0.26234605 + 5.7i(-4)$
40	$0.26400465 - 5.0i(-6)$	$0.26400457 - 5.0i(-6)$
60	$0.26400174 - 3.2i(-9)$	$0.26400166 + 1.3i(-8)$
80	$0.26400174 - 3.0i(-9)$	$0.26400166 + 1.3i(-8)$
100	$0.26400174 - 3.0i(-9)$	$0.26400166 + 1.3i(-8)$
120	$0.26400174 - 3.0i(-9)$	$0.26400166 + 1.3i(-8)$

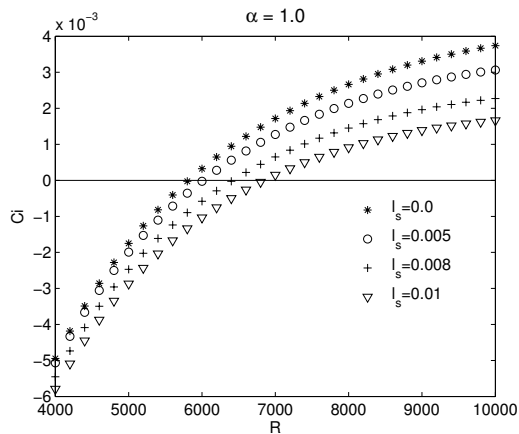


Fig. 1 The largest imaginary part C_i as a function of Reynolds number for four different values of slip length. Here $\alpha = 1.0$.

Table 6 Approximation to the eigenvalue with largest imaginary part at the critical Reynolds number and wave number $\alpha_c = 0.9922$, when $l_s = 0.008$, by the Chebyshev method.

grid points N	$\lambda(R = 6410.91)$	$\lambda(R = 6410.92)$
20	$0.25993871 - 2.3i(-3)$	$0.25993866 - 2.3i(-3)$
40	$0.26159407 - 3.2i(-5)$	$0.26159400 - 3.2i(-5)$
60	$0.26159987 + 1.1i(-8)$	$0.26159980 + 2.4i(-8)$
80	$0.26159988 - 1.4i(-9)$	$0.26159981 + 1.2i(-8)$
100	$0.26159988 - 1.4i(-9)$	$0.26159981 + 1.2i(-8)$
120	$0.26159988 - 1.4i(-9)$	$0.26159981 + 1.2i(-8)$

One can also calculate the critical Reynolds number for different wave number α and plot the neutral stable curves. Fig. 2 plots the neutral stable curves (critical Reynolds number as a function of wave number α) for increasing slip length at $l_s = 0, 0.005, 0.008$, and 0.01 .

For each fixed slip length, the neutral stable curve first decreases with the wave number α and then start to increase when α is large enough due to viscosity which dumps the high frequency disturbance.

It is clear that the critical Reynolds number R_c increases from about 5772 to about 6011, 6411, and 6778, respectively. However, the most unstable wave numbers α_c decreases (i.e. shifting to the left).

To study quantitatively how the critical Reynolds number R_c on the slip length l_s , we plot in Fig. 3 the $(R_c(l_s) - R_c(0))/R_c(0)$ versus l_s on log-log scale. Here $R_c(0)$ is the critical Reynolds number corresponding to no-slip boundary

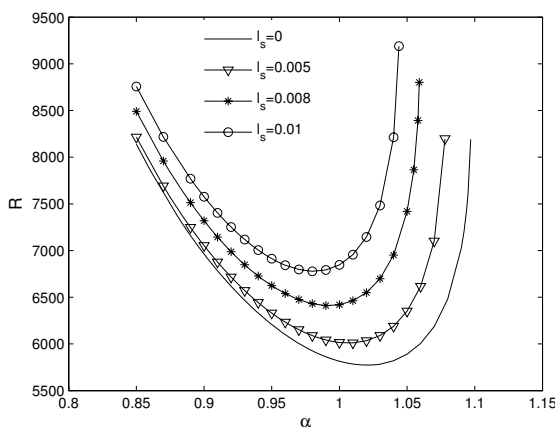


Fig. 2 The neutral stability curves for increasing slip length.

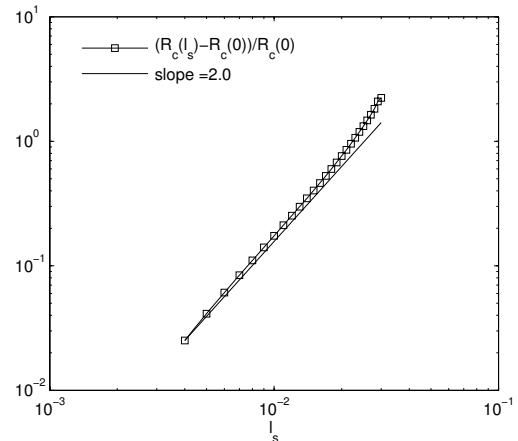


Fig. 3 Log-log plot of $(R_c(l_s) - R_c(0))/R_c(0)$ versus l_s . For comparison, the solid line is the log-log plot for $y = l_s^2$.

conditions. Measurement of the slope of the curve suggests that we have

$$\frac{R_c(l_s) - R_c(0)}{R_c(0)} \approx l_s^2.$$

5 Conclusions

We study the linearized stability of the shear flow with Navier slip boundary conditions. The corresponding Orr-Sommerfeld equation is numerically solved to study the spectra and stability of the plane Poiseuille flow. Our results show that allowing slip at the wall increases the critical Reynolds number and the flow becomes more stable. It is also shown that the dependence of the critical Reynolds number on the slip length is weak and $R_c(l_s) - R_c(0) \approx Cl_s^2$.

Acknowledgements This work is supported in part by Hong Kong RGC Central Allocation Grant CA05/06.SC01 and RGC-DAG 04/05.sc17.

References

- [1] P. G. Drazin and W. H. Reid, *Hydrodynamics stability* (Cambridge University Press, London 1981).
- [2] S. A. Orszag, Accurate solution of the Orr-Sommerfeld equation, *J. Fluid Mech.* **50**, 689–703 (1971).
- [3] S. J. Davies and C. M. White, An experimental study of the flow in pipes of rectangular section, *Proc. R. Soc. Lond. A* **119**, 92 (1982).
- [4] J. K. Platten and J. C. Legros, *Convection in Liquids* (Springer, Berlin, 1984).
- [5] V. C. Patel and M. R. Head, Some observations on skin friction and velocity profiles in fully developed pipe and channel flows, *J. Fluid Mech.* **38**, 181–201 (1969).
- [6] Z. K.-H. Chu, Note on spectra from the relaxed boundary conditions, *Z. Angew. Math. Mech.* **81**(3), 211–215 (2001).
- [7] F. Li and S. E. Widnall, Wave patterns in plane Poiseuille flow created by concentrated disturbances, *J. Fluid Mech.* **208**, 639–656 (1989).
- [8] K.-H. Chu and C.-C. Chang, A new approach for the spectrum of Orr-Sommerfeld equation, in: *Proceedings of the Aero. and Astro. Conf., Aeronautical and Astronautical Society of the republic of China, Taipei 1990*, pp. 199–202.
- [9] A. Kundt and E. Warburg, Über Reibung und Wärmeleitung verdünnter Gase, *Pogg. Ann. Phys.* **156**, 177 (1875); **20**, 1–14 (1969).
- [10] Tiezheng Qian, Xiao-Ping Wang, and Ping Sheng, A variational approach to the moving contact line hydrodynamics, *J. Fluid Mech.* **564**, 333–360 (2006).
- [11] Tie-Zheng Qian and Xiao-Ping Wang, Driven cavity flow: from molecular dynamics to continuum hydrodynamics, *SIAM J. Multiscale Modeling and Simulation* **3**, 749–763 (2005).
- [12] L. H. Thomas, The stability of plane Poiseuille flow, *Phys. Rev.* **91**(4), 780–783 (1953).
- [13] J. A. C. Weideman and S. C. Reddy, A MATLAB differentiation matrix suite, *ACM Trans. Math. Software* **26**(4), 465–519 (2000).